Spectroscopic ellipsometry of homoepitaxial diamond multilayers and delta-doped structures

Jessica Bousquet, Gauthier Chicot, David Eon, Etienne Bustarret

▶ **To cite this version:**

Jessica Bousquet, Gauthier Chicot, David Eon, Etienne Bustarret. Spectroscopic ellipsometry of homoepitaxial diamond multilayers and delta-doped structures. Applied Physics Letters, 2014, 104 (2), pp.021905. 10.1063/1.4861860 . hal-00932150

HAL Id: hal-00932150
https://hal.science/hal-00932150

Submitted on 17 Jan 2014

HAL is a multi-disciplinary open access archive for the deposit and dissemination of scientific research documents, whether they are published or not. The documents may come from teaching and research institutions in France or abroad, or from public or private research centers.

L'archive ouverte pluridisciplinaire **HAL**, est destinée au dépôt et à la diffusion de documents scientifiques de niveau recherche, publiés ou non, émanant des établissements d'enseignement et de recherche français ou étrangers, des laboratoires publics ou privés.

Spectroscopic ellipsometry of homoepitaxial diamond multilayers and delta-doped structures

J. Bousquet,[1,2] G. Chicot,[1,2] D. Eon,[1,2] and E. Bustarret[1,2]
[1]*Univ. Grenoble Alpes, Inst. NEEL, F-38042 Grenoble, France*
[2]*CNRS, Inst. NEEL, F-38042 Grenoble, France*

(Received 20 October 2013; accepted 28 December 2013; published online 14 January 2014)

The optimization of diamond-based unipolar electronic devices such as pseudo-vertical Schottky diodes or delta-doped field effect transistors relies in part on the sequential growth of nominally undoped (p^-) and heavily boron doped (p^{++}) layers with well-controlled thicknesses and steep interfaces. Optical ellipsometry offers a swift and contactless method to characterize the thickness, roughness, and electronic properties of semiconducting and metallic diamond layers. We report ellipsometric studies carried out on delta-doped structures and other epitaxial multilayers with various boron concentrations and thicknesses (down to the nanometer range). The results are compared with Secondary Ion Mass Spectroscopy and transport measurements. © *2014 AIP Publishing LLC*. [http://dx.doi.org/10.1063/1.4861860]

Spectroscopic ellipsometry has been introduced quite early on as an efficient way of characterizing the nucleation and subsequent coalescence and growth of polycrystalline diamond on silicon substrates induced by chemical vapor deposition (CVD), either *in situ*[1–7] or *ex situ*.[8–13] The main ingredients of this approach were the optical transparency of diamond in the visible range and the sizable difference between the refractive index of diamond (around 2.4) and that of the silicon substrate (around 3.5) over this spectral range.[14] In the case of homoepitaxial growth, no such discontinuity was expected between film and substrate, so that equivalent studies have not been published. Actually, in contrast to other semiconductors, spectrometric ellipsometry has not been a popular way to determine optical constants of single crystal diamond. Indeed, even in the ultraviolet region, close to the direct gap, artefacts most probably related to the surface roughness of the polished crystals may well have affected the few reported values.[15,16]

However, at the heavy boron doping levels leading to metallic properties in diamond (above 4×10^{20} [B]/cm^3 (Ref. 17)), a noticeable change in refractive index has been detected by reflectance spectroscopy,[18] first in the mid-infrared, then up to the near ultraviolet range.[19] As confirmed by other studies in the far infrared,[20] the contribution of free holes was fairly well described by an additional Drude component to the pseudo dielectric function of diamond, and the change of refractive index could be evaluated over the whole spectral range. A consequence of this observation is that stacks of well-defined metallic (p^{++}) and semiconducting (p^- or p) layers are expected to have spectral characteristics in the visible range that could be measured and simulated as those of any optical multilayer, providing an access to their respective thickness and electronic microscopic properties at optical frequencies. Such epitaxial metallic diamond layers of micrometric to nanometric thickness, which have been proposed as buried electrical contacts for both n/i/p and Schottky pseudo-vertical devices,[21–23] as source and drain in field effect transistors (FET) or even as a pseudo-channel[24] in delta-doped metal-insulator semiconductor FETs, have been recently investigated, and new results about their chemical profiles[25–27] or temperature-dependent transport properties[26,28,29] have been published. It is the purpose of the present letter to show that spectroscopic ellipsometry provides a time-effective but yet powerful characterization of metallic layers or alternating p^-/p^{++} epitaxial diamond multilayers similar (before patterning) to those involved in the monolithic devices mentioned above.

To this aim, we have studied the ellipsometric response of various diamond homoepitaxial stacks, including uncapped and capped delta-doped structures and two series of p^{++} epilayers where either the thickness or the doping level were varied. We report the experimental spectra and their fits with standard model dielectric functions specific to each epilayer. Thicknesses, optically determined room temperature resistivities, and carrier concentrations will then be compared with Secondary Ion Mass Spectroscopy (SIMS) and DC transport measurements.

A TE_{10} standing microwave field was obtained in a rectangular waveguide of a microwave plasma-assisted CVD (MPCVD) reactor where the reaction chamber composed of a quartz tube was positioned at a maximum of the electric field. The $H_2 + CH_4$ plasma was ignited close to the diamond substrate, which was held at 910 °C for the non intentionally doped p^- layers, and at 830 °C for heavily boron doped (p^{++}) growth resulting from adding diborane (B_2H_6) to the gas mixture. The total flow rate was kept to 100 sccm at a pressure of 40 mbar. Three sets of samples were grown, labeled as "thickness," "doping," and "capped." The "thickness" series involved p^{++} layers where only the growth duration was changed between 1 and 60 min (CH_4/H_2 molar ratio of 4%, B_2H_6/CH_4 molar ratio 600 ppm) resulting in epilayers thicknesses ranging from 30 to 1800 nm. The samples of the "doping" series are p^{++} layers about 1 μm-thick where the diborane to methane ratio was varied between 150 and 6000 ppm leading to solid state concentrations ranging[17,30] from 2×10^{20} and 2×10^{21} [B]/cm^3. The samples of these two series were considered as metallic at room temperature. The third set involved three samples where the p^{++} layer was overgrown with a p^- "cap layer" (CL). For one sample dubbed "thick stack," the growth

 © 2014 AIP Publishing LLC

This article is copyrighted as indicated in the article. Reuse of AIP content is subject to the terms at: http://scitation.aip.org/termsconditions. Downloaded to IP: 147.173.64.73 On: Tue, 14 Jan 2014 16:19:09

conditions of the p^{++} layer were those of the thickness series, and the resulting p^{++} and cap p^{-} epilayer were a few μm-thick. For the other two samples dubbed "delta 1" and "delta 2," the conditions were changed, with CH_4/H_2 and B_2H_6/CH_4 molar ratios in the gas phase of 0.5% and 3000 ppm, respectively, while the total pressure was raised to 67 mbar and the total flow rate to 2 slm in order to reduce the residence time of the gas species. Under these conditions, the growth rate decreased from typically 30 to 6 nm/min and much thinner epilayers were grown. Additionally, as described elsewhere,[29,31] $O_2 + H_2$ gas mixtures were used to etch *in situ* the ultra-thin p^{++} layers down to the required thickness without turning off the plasma.

Spectroscopic ellipsometry was performed with a J.A. Woollam M2000 ellipsometer running under the CompleteEase software. The ellipsometric angles (Ψ, Δ) defined by the ratio of the reflection coefficients for electric fields, respectively, parallel (p) and perpendicular (s) to the incidence plane ($r_p/r_s = \tan(\Psi)e^{i\Delta}$) were acquired over the 240–1000 nm wavelength range at a 75° incidence angle. These data were simulated using a Cauchy model for the optical constants of diamond in the case of non-intentional doped layers or substrates, and adding a Drude component to UV oscillators for metallic layers. Contrary to the epitaxial layers, the 0.3 to 0.5 mm-thick undoped [100]-oriented diamond substrate (either type-Ib or type IIa optical grade crystals) was described as an incoherent optical layer where only the intensities of the multiple reflected beams should be summed (instead of amplitudes). A random surface roughness parameter (in nm) was also introduced in the simulation, for the top surface only.

To perform Hall effect measurements, the cap and the delta-doped layers have been delineated by Reactive Ion Etching to fabricate a Hall bar. Ohmic contacts have been fabricated by annealing at 750 °C under vacuum ($<10^{-8}$ mbar) during 30 min the Ti/Pt/Au pads. The sheet carrier density measurements have been carried out at room temperature in vacuum with a DC magnetic field (amplitude of 0.8 T) in the standard configuration (magnetic field parallel and current density perpendicular to the growth axis [100]). In some cases, four terminal silver paste resistivity measurements have also been performed.

The metallic layer optical response has been fitted by adding a Drude component to the interpolated dielectric function ε_{nid} of undoped diamond[14]

$$\varepsilon(\omega) = \varepsilon_{nid}(\omega) + i\frac{Ne^2\tau}{\varepsilon_0 m_0 m^*}\frac{\omega}{1 - i\omega\tau}, \quad (1)$$

with ω the wavenumber (or reciprocal wavelength $1/\lambda$), N the free carriers (here holes) concentration, τ the scattering time, e the elementary electron charge, m_0 the electron rest mass and m* the relative effective mass of the holes. Beside the thickness d of the p^{++} layer, and the top surface roughness, the two fit parameters were the relaxation time τ and the N/m* ratio. This simple relaxation time approximation of a Fermi metal provides a direct access to the optical resistivity at zero frequency

$$\rho(\omega) = \rho_0(1 - i\omega\tau) = \frac{m_0 m^*}{Ne^2\tau}(1 - i\omega\tau). \quad (2)$$

TABLE I. Correlation table for the fit of both ellipsometric angles measured on sample delta-1. The influence of strongly correlated parameters (correlation coefficient close to ± 1) cannot be disentangled.

	d	d_{CL}	ρ	τ
d	1	−0.8	0.1	−0.9
d_{CL}	−0.8	1	0.3	0.9
ρ	0.1	0.3	1	−0.1
τ	−0.9	0.9	−0.1	1

After each fit, beside the overall minimum mean square deviation (MSE), a table was calculated showing the correlation coefficients (from 0, no correlation, to 1, fully correlated) between the fit parameters corresponding to the various layers of the stack (see Table I).

As shown in Fig. 1(a), in the case of an optically thick p^{++} film (no reflected light coming from the back interface) the spectral dependence of the two ellipsometric angles Ψ and Δ was measured and then simulated by the optical response of a rough semi-infinite medium with a complex wavelength-dependent pseudodielectric function $\varepsilon(\lambda)$ or refractive index $n(\lambda)+ik(\lambda)$. A similar approach can be applied to polished insulating bulk diamond.

In the case of commercial diamond substrates, the fitted pseudodielectric functions taking their roughness into account lie close to those deduced from the n and k values found in a classical handbook,[14] which were as usual readily interpolated over the present spectral range by a Cauchy law.[14] The real part n of the refractive index was found slightly higher in yellow type Ib substrates grown at high pressure and high temperature (HPHT) than in optical grade

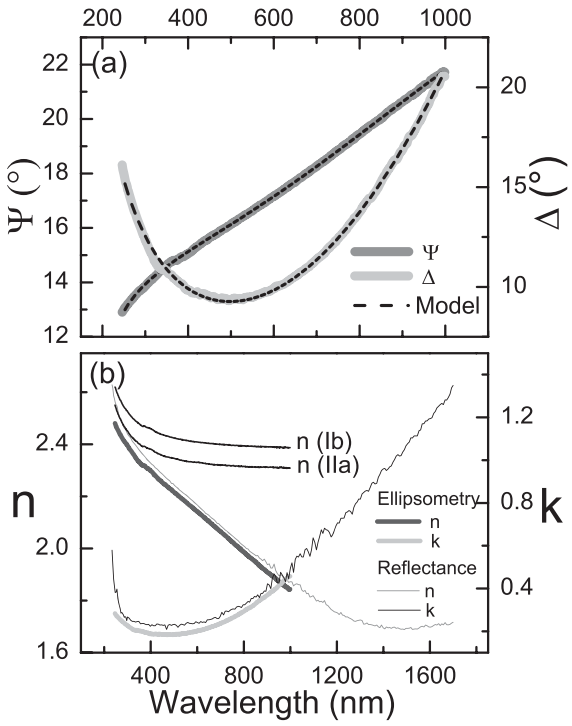

FIG. 1. (a) Spectral variation of the ellipsometric angles for an optically thick p^{++} diamond layer. (b) Optical indices deduced from (a), compared with reflectometry measurements and the refractive index of type-Ib (HPHT) and type-IIa (CVD) diamond substrates.

This article is copyrighted as indicated in the article. Reuse of AIP content is subject to the terms at: http://scitation.aip.org/termsconditions. Downloaded to IP: 147.173.64.73 On: Tue, 14 Jan 2014 16:19:09

CVD substrates (Fig. 1(b)). This can be explained by the high density of isolated Nitrogen in the Ib substrates leading to an optical absorption above 1.7 eV (below 729 nm). In the case of the thick metallic diamond layer, in order to obtain satisfactory simulations, it was necessary to add to $\varepsilon(\lambda)$ of undoped diamond a Drude component[17] parameterized here by the zero frequency limit ρ_0 of the frequency-dependent optical resistivity and by the microscopic relaxation time τ, as defined above. The experimental optical constants n and k are shown in Fig. 1(b) to be very similar to those previously published for similar films,[18] with a real part n becoming significantly weaker than in undoped diamond at longer wavelengths. This sizable contrast in refractive index (−20% at 1 μm wavelength) between insulating (or p^-) and metallic (p^{++}) diamond led us to study optically various stacks of p^- and p^{++} epilayers.

The first case that comes to mind is that of uncapped and thin metallic diamond films grown on commercial substrates, similar to those used in superconductivity[27] or delta-doping[25,32] studies. The spectral dependence of the ellipsometric angles for two such films ("thickness series") is given in Figs. 2(a) and 2(b), with best fit simulations of the Fabry-Perot fringes yielding thicknesses d of 29 nm and 167 nm for

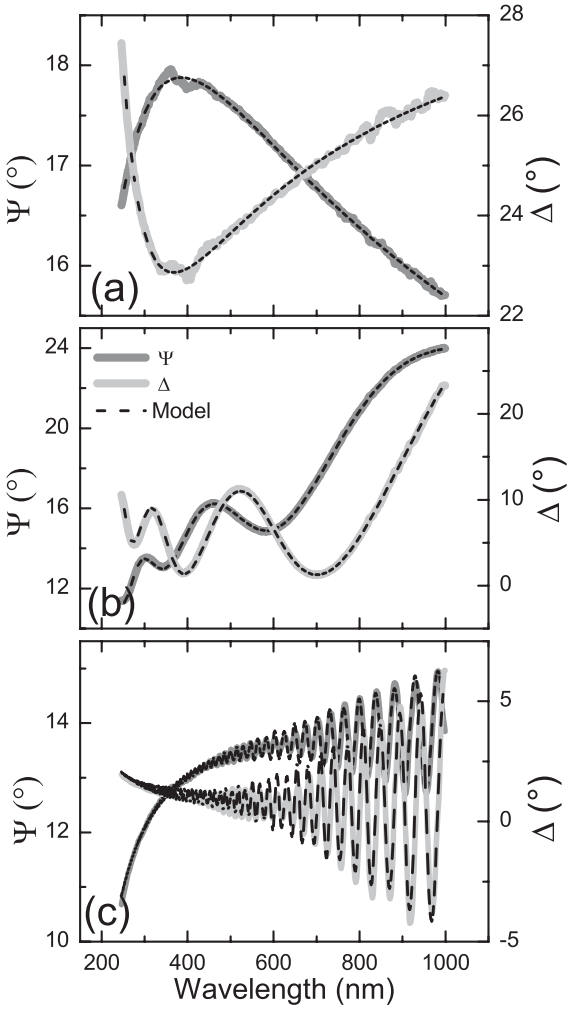

FIG. 2. Spectral dependence of the experimental and simulated ellipsometry parameters for a (a) 29 nm- and (b) 167 nm-thick uncapped p^{++} layer and (c) a bilayer p^-/p^{++} stack.

1 and 5 min growth times, within 10% of the thicknesses expected from the nominal deposition rate of 31 nm/min. A third example is given on Fig. 2(c), that of a "thick stack" involving a p^- layer grown on top of a p^{++} layer grown on a commercial CVD substrate. The amplitude of the fringes is smaller, mostly because of an increased surface roughness, but still determined by the contrast in refractive index, which increases with the wavelength. The thicknesses resulting from the fit, $d = 1.5\,\mu$m for the p^{++} bottom layer, and $d_{CL} = 3.8\,\mu$m for the top p^- cap layer, were also within 10% of the values expected from previous boron concentration SIMS and neutron depth profiles.[30] Because the present spectral range was limited to 1 μm in the infrared, the maximum thicknesses measurable in this non-destructive way for such bilayers were $d_{CL} = 8\,\mu$m for the top p^- cap layer and $d = 2\,\mu$m for the underlying p^{++} epilayer.

In the case of uncapped metallic diamond epilayers, as shown in Fig. 3(a), the reliability of the thickness values deduced from ellipsometry spectra was confirmed over almost two orders of magnitude for the whole "thickness series." Over this series, the ρ_0 value deduced from the best fit for each of these samples was almost constant. Once multiplied by the optically determined thickness d, an average optical sheet resistivity was determined, and compared in Fig. 3(b) to the DC value measured at room temperature by the 4-terminal probe method. In both cases the −1 slope of the log-log plot was compatible with a constant resistivity value over the whole thickness range. This resistivity value was 2.4 mΩ.cm for DC measurements, higher than extrapolated from the optical data (1.7 mΩ.cm). This discrepancy was tentatively

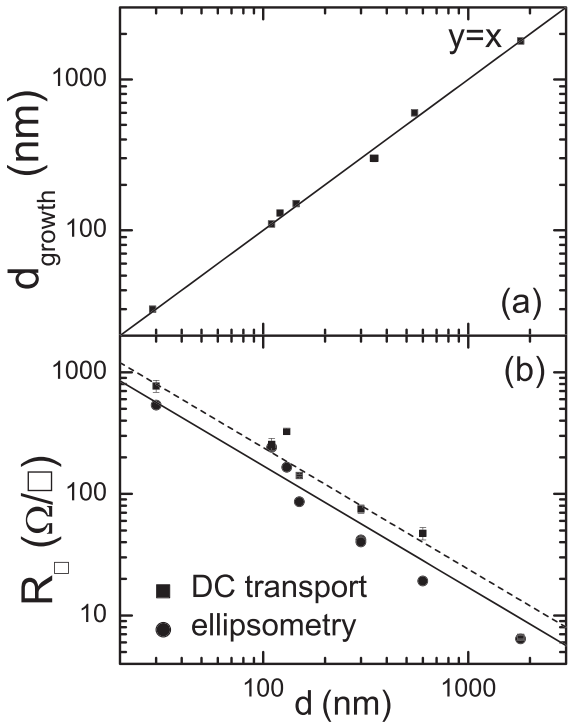

FIG. 3. (a) Thickness expected from the growth rate, as a function of the optically determined thickness. The solid line corresponds to a constant growth rate of 31 nm/min. (b) Thickness dependence of the sheet resistance deduced from spectroscopic ellipsometry and DC measurements. The straight and the dashed lines correspond to average resistivity values of 1.7 and 2.4 mΩ.cm.

This article is copyrighted as indicated in the article. Reuse of AIP content is subject to the terms at: http://scitation.aip.org/termsconditions. Downloaded to IP: 147.173.64.73 On: Tue, 14 Jan 2014 16:19:09

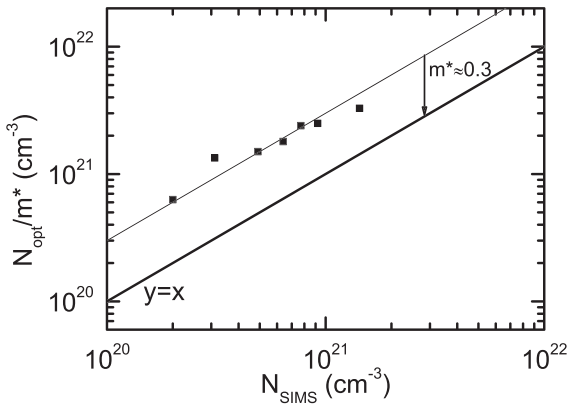

FIG. 4. Normalized free carrier concentration deduced from ellipsometry as a function of the boron concentration deduced from SIMS profiles of μm-thick films ("doping" series).

attributed to the limited optical spectral range which did not extend far enough below the plasmon edge to take into account scattering events occurring at lower frequencies.

Spectroscopic ellipsometry was also performed on the "doping series" of epilayers. We used the N/m* ratio as a parameter of the Drude model and compared in Fig. 4 the results to the boron concentration previously determined[29,30] by SIMS. The carrier concentrations deduced from ellipsometry seemed be significantly higher than the boron concentration, as observed previously for optical[18] as well as Hall effect measurements.[18,29] If, however, the optical mass was fixed at 0.3 m_0, the agreement became acceptable. This value is much lower than the optical effective mass 0.74 m_0 which has been deduced from the optical excitation spectrum of the boron acceptor.[33]

For reasons explained elsewhere,[23,28,34,35] we also undertook the study of two delta-doped structures made of a few nm-thick metallic layer overgrown with a few tens of nm-thick p^- doped cap layer (delta-1 and delta-2). The spectral dependence of the ellipsometric angles was simulated yielding nominal thicknesses of, respectively, 3 nm and 1.3 nm for the metallic films and 36 nm and 28 nm for the cap layers (lowest MSE). As illustrated by Fig. 5, the

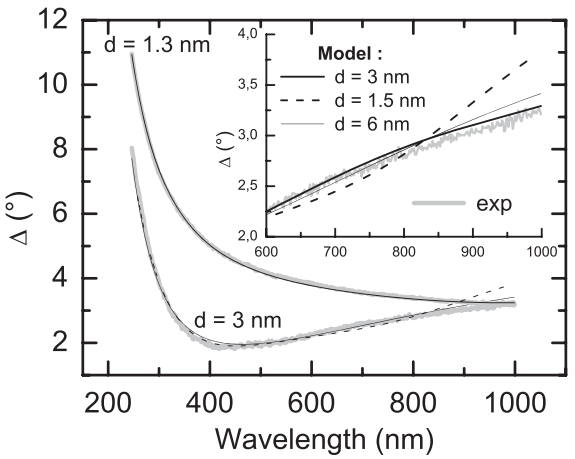

FIG. 5. Fitted and experimental spectral dependence of Δ angle for delta-1 and delta-2 samples. Models for delta-1 at nominal thickness (d = 3 nm) and other fixed values (d = 1.5 nm and d = 6 nm) are presented. Inset: details of the delta-1 spectra in the near infrared region.

experimental Δ spectra was reproduced almost equally well by a set of pairs of geometrical thicknesses d and d_{CL}. For example, the fit of the delta-1 sample obtained for d = 3 nm and d_{CL} = 36.5 nm is only slightly better than the one using d = 6 nm and d_{CL} = 33.5 nm or, for that matter, than the simulation assuming d = 1.5 nm and d_{CL} = 39 nm. As shown by the inset of Fig. 5, the fit was more sensitive in the near-infrared region of the spectrum, so that an extension to longer wavelengths should reduce this uncertainty. The fact that these two fitting parameters are far from being independent from one another is also illustrated by Table I, where the corresponding values of the correlation coefficients are close to unity.

However, while the resistivity ρ_0 value of the Drude metal affected the simulation quite independently of both thicknesses values, Table I also shows that the latter were strongly correlated to the scattering time value. An extension of the spectral range of the ellipsometer to the infrared should increase the sensibility of the measurements to the optical absorption attributed to the free carriers, and thus lower the correlation coefficients.

In conclusion, we have shown that spectroscopic ellipsometry is a powerful non-destructive tool to probe the thicknesses, the optical parameters and the electronic properties of semiconducting and metallic single crystal diamond epilayers and multilayers. Two series of uncapped metallic epilayers with either various boron concentrations or various thicknesses have been grown and measured. Thicknesses and sheet resistance values deduced from the simulations were close to those expected from the growth rate and DC four points probe measurements. A similar agreement between carrier concentrations extracted from the simulations and boron concentrations deduced from SIMS profiles was obtained assuming an optical mass of about 0.3 m_0. Spectroscopic ellipsometry was also performed on two capped delta-doped layers with thicknesses in the nm range. The simulation of the spectra was found much more sensitive to the sum rather than to the individual values of the delta layer and the cap layer thicknesses. Moreover, the strong correlation of those two parameters with the scattering time deduced from the Drude model limited the precision on the delta layer thickness and electronic properties. We suggest that this situation would be significantly improved by extending the spectral range of the spectrometer to the infrared.

The authors would like to acknowledge the significant contribution of Dr. P. Achatz who grew some of the thicker p^{++} samples. This work was partially supported by the French FUI project "DiamondX2."

[1]R. W. Collins, Y. Cong, Y.-T. Kim, K. Vedam, Y. Liou, A. Inspektor, and R. Messier, Thin Solid Films **181**, 565 (1989).
[2]R. W. Collins, Y. Cong, H. V. Nguyen, I. An, K. Vedam, T. Badzian, and R. Messier, J. Appl. Phys. **71**, 5287 (1992).
[3]Y. Hayashi, W. Drawl, R. W. Collins, and R. Messier, Appl. Phys. Lett. **60**, 2868 (1992).
[4]Y. Hayashi, X. Li, and S. Nishino, Appl. Phys. Lett. **71**, 2913 (1997).
[5]B. Hong, J. Lee, R. W. Collins, Y. Kuang, W. Drawl, R. Messier, T. T. Tsong, and Y. E. Strausser, Diamond Relat. Mater. **6**, 55 (1997).
[6]J. Lee, P. I. Rovira, I. An, and R. W. Collins, Appl. Phys. Lett. **72**, 900 (1998).

This article is copyrighted as indicated in the article. Reuse of AIP content is subject to the terms at: http://scitation.aip.org/termsconditions. Downloaded to IP: 147.173.64.73 On: Tue, 14 Jan 2014 16:19:09

[7]J. Lee, B. Hong, R. Messier, and R. W. Collins, Thin Solid Films **313–314**, 506 (1998).
[8]Y. Cong, R. W. Collins, G. F. Epps, and H. Windischmann, Appl. Phys. Lett. **58**, 819 (1991).
[9]N. Cella, H. E. Rhaleb, J. P. Roger, D. Fournier, E. Anger, and A. Gicquel, Diamond Relat. Mater. **5**, 1424 (1996).
[10]I. Pintér, P. Petrik, E. Szilagui, Sz. Katai, and P. Deak, Diamond Relat. Mater. **6**, 1633 (1997).
[11]S. Gupta, B. R. Weiner, and G. Morell, J. Appl. Phys. **90**, 1280 (2001).
[12]S. Gupta, A. Dudipala, O. A. Williams, K. Haenen, and E. Bohannan, J. Appl. Phys. **104**, 073514 (2008).
[13]A. Zimmer, O. A. Williams, K. Haenen, and H. Terryn, Appl. Phys. Lett. **93**, 131910 (2008).
[14]D. E. Edwards and H. R. Philipp, in *Handbook of Optical Constants of Solids*, edited by E. Palik (Academic Press Inc. 1985), pp. 665–673.
[15]S. Logothetidis, J. Petalas, H. M. Polatoglou, and D. Fuchs, Phys. Rev. B **46**, 4483 (1992).
[16]N. Kumagai, S. Yamazaki, and H. Okushi, Diamond Relat. Mater. **13**, 2092 (2004).
[17]T. Klein, P. Achatz, J. Kacmarcik, C. Marcenat, F. Gustafsson, J. Marcus, E. Bustarret, J. Pernot, F. Omnès, B. E. Sernelius, C. Persson, A. F. da Silva, and C. Cytermann, Phys. Rev. B **75**, 165313 (2007).
[18]E. Bustarret, F. Pruvost, M. Bernard, C. Cytermann, and C. Uzan–Saguy, Phys. Status Solidi A **186**, 303 (2001).
[19]E. Bustarret, E. Gheeraert, and K. Watanabe, Phys. Status Solidi A **199**, 9 (2003).
[20]M. Ortolani, S. Lupi, L. Baldassare, U. Schade, P. Calvani, Y. Takano, M. Nagao, T. Takenouchi, and H. Kawarada, Phys. Rev. Lett. **97**, 097002 (2006).
[21]T. Makino, S. Tanimoto, Y. Hayashi, H. Kato, N. Tokuda, M. Ogura, D. Takeuchi, K. Oyama, H. Ohashi, H. Okushi, and S. Yamasaki, Appl. Phys. Lett. **94**, 262101 (2009).
[22]A. Nawawi, K. J. Tseng, Rusli, G. A. J. Amaratunga, H. Umezawa, and S. Shikata, Diamond Relat Mater. **35**, 1 (2013).
[23]H. Umezawa, Y. Kato, and S. Shikata, Appl. Phys. Express **6**, 011302 (2013).
[24]R. S. Balmer, I. Friel, S. M. Woolard, C. J. H. Wort, G. A. Scarsbrook, S. E. Coe, H. El-Hajj, A. Kaiser, A. Denisenko, E. Kohn, and J. Isberg, Philos. Trans. R. Soc., A **366**, 251 (2008).
[25]Y. G. Lu, S. Turner, J. Verbeek, S. D. Janssens, P. Wagner, K. Haenen, and G. Van Tendeloo, Appl. Phys. Lett. **101**, 041907 (2012).
[26]R. S. Balmer, I. Friel, S. Hepplestone, J. Isberg, M. J. Uren, M. L. Markham, N. L. Palmer, J. Pilkington, P. Huggett, S. Madji, and R. Lang, J. Appl. Phys. **113**, 033702 (2013).
[27]A. Fiori, F. Jomard, T. Teraji, S. Koizumi, J. Isoya, E. Gheeraert, and E. Bustarret, Appl. Phys. Express **6**, 045801 (2013).
[28]S. Kitagoh, R. Okada, A. Kawano, M. Watanabe, Y. Takano, T. Yamaguchi, T. Chikyow, and H. Kawarada, Physica C **470**, S610 (2010).
[29]G. Chicot, T. N. T. Thi, A. Fiori, F. Jomard, E. Gheeraert, E. Bustarret, and J. Pernot, Appl. Phys. Lett. **101**, 162101 (2012).
[30]P. Achatz, F. Omnès, L. Ortéga, C. Marcenat, J. Vacik, V. Hnatowicz, U. Köster, F. Jomard, and E. Bustarret, Diamond Relat. Mater. **19**, 814 (2010).
[31]A. Fiori, T. N. T. Thi, G. Chicot, F. Jomard, F. Omnès, E. Gheeraert, and E. Bustarret, Diamond Relat. Mater. **24**, 175 (2012).
[32]R. Edgington, S. Sato, Y. Ishiyama, R. Morris, R. B. Jackman, and H. Kawarada, J. Appl. Phys. **111**, 033710 (2012).
[33]E. Gheeraert, S. Koizumi, T. Teraji, H. Kanda, and M. Nesladek, Phys. Status Solidi A **174**, 39 (1999).
[34]A. Fiori, J. Pernot, E. Gheeraert, and E. Bustarret, Phys. Status Solidi A **207**, 2084 (2010).
[35]H. El-Hajj, A. Denisenko, A. Kaiser, R. S. Balmer, and E. Kohn, Diamond Relat. Mater. **17**, 1259 (2008).

This article is copyrighted as indicated in the article. Reuse of AIP content is subject to the terms at: http://scitation.aip.org/termsconditions. Downloaded to IP: 147.173.64.73 On: Tue, 14 Jan 2014 16:19:09